Memory Enhancement by Targeting Cdk5 Regulation of NR2B

Florian Plattner,[1,8] Adan Hernández,[1,8] Tara M. Kistler,[1,8] Karine Pozo,[1] Ping Zhong,[2] Eunice Y. Yuen,[2] Chunfeng Tan,[1] Ammar H. Hawasli,[1] Sam F. Cooke,[3] Akinori Nishi,[4] Ailan Guo,[5] Thorsten Wiederhold,[5] Zhen Yan,[2] and James A. Bibb[1,6,7,*]

[1]Department of Psychiatry, The University of Texas Southwestern Medical Center, Dallas, TX 75390, USA
[2]Department of Physiology and Biophysics, State University of New York at Buffalo, Buffalo, NY 14214, USA
[3]Picower Institute for Learning and Memory, Massachusetts Institute of Technology, Cambridge, MA 02139, USA
[4]Department of Pharmacology, School of Medicine, Kurume University, Fukuoka 830-0011, Japan
[5]Cell Signaling Technology, CNS Development, Danvers, MA 01923, USA
[6]Department of Neurology and Neurotherapeutics, The University of Texas Southwestern Medical Center, Dallas, TX 75390, USA
[7]Harold C. Simmons Comprehensive Cancer Center, The University of Texas Southwestern Medical Center, Dallas, TX 75390, USA
[8]These authors contributed equally to this work
*Correspondence: james.bibb@utsouthwestern.edu
http://dx.doi.org/10.1016/j.neuron.2014.01.022

SUMMARY

Many psychiatric and neurological disorders are characterized by learning and memory deficits, for which cognitive enhancement is considered a valid treatment strategy. The N-methyl-D-aspartate receptor (NMDAR) is a prime target for the development of cognitive enhancers because of its fundamental role in learning and memory. In particular, the NMDAR subunit NR2B improves synaptic plasticity and memory when overexpressed in neurons. However, NR2B regulation is not well understood and no therapies potentiating NMDAR function have been developed. Here, we show that serine 1116 of NR2B is phosphorylated by cyclin-dependent kinase 5 (Cdk5). Cdk5-dependent NR2B phosphorylation is regulated by neuronal activity and controls the receptor's cell surface expression. Disrupting NR2B-Cdk5 interaction via a small interfering peptide (siP) increases NR2B surface levels, facilitates synaptic transmission, and improves memory formation in vivo. Our results reveal a regulatory mechanism critical to NR2B function that can be targeted for the development of cognitive enhancers.

INTRODUCTION

N-methyl-D-aspartate receptors (NMDARs) are ionotropic glutamate receptors that exhibit broad expression within the nervous system and are critically involved in neuronal processes such as synaptic plasticity and learning and memory (Bliss and Collingridge, 1993; Martin et al., 2000). Functional NMDARs are obligate heterotetrameric complexes formed by two glycine-binding GluN1 subunits assembled with two of several isoforms of the glutamate-binding GluN2 (A, B, C, or D subtypes) or glycine-binding GluN3 (A or B subtypes) (Cull-Candy and Leszkiewicz, 2004; Dingledine et al., 1999). The biophysical properties of NMDARs are dependent on their subunit composition (Morrisett, 1997). Indeed, NMDAR subunit composition varies greatly between different synapses and neurons, as well as during neuronal development (Monyer et al., 1994; Sheng et al., 1994). Therefore, precise spatiotemporal regulation of NMDAR subunit expression, composition, trafficking, and localization is critical for proper neuronal function.

Brain regions involved in mnemonic functions rely predominantly upon GluN2A (NR2A) and GluN2B (NR2B) subunit-containing NMDARs. During postnatal development, NR2B expression steadily decreases, whereas NR2A levels rise. Compared to NR2A-containing NMDARs, receptors that include NR2B inactivate more slowly and, consequently, have been associated with increased levels of synaptic plasticity (Cull-Candy and Leszkiewicz, 2004; Lau and Zukin, 2007). Consistently, upregulation of NR2B expression in mice improves synaptic plasticity and memory formation (Crair and Malenka, 1995; Tang et al., 1999). Numerous animal models that feature elevated NR2B levels via altered synthesis, transport, or degradation exhibit improved synaptic plasticity and memory (Lee and Silva, 2009). Hence, targeting NR2B and its regulatory machinery has been singled out as an attractive approach for cognitive enhancement (Bibb et al., 2010; Collingridge et al., 2013).

One possible strategy to increase NR2B levels involves induction of its de novo synthesis, for example, via cAMP response element (CRE)-mediated gene expression or chromatin remodeling (Fujita et al., 2012; Jiang et al., 2010; Myers et al., 1999). Alternative targets include transport or degradation of NR2B via its coupling to distinct intracellular signaling pathways (Hawasli et al., 2007; Yin et al., 2011). The molecular machinery regulating trafficking, subcellular localization, and degradation of NMDAR subunits is not yet well understood, but it has been recognized that phosphorylation of NMDAR subunits including NR2B is important for the regulation of such processes (Chen and Roche, 2007; Ma and Jan, 2002; Wenthold et al., 2003). One protein kinase implicated in the metabolism of NR2B is Cdk5 (Cyclin-dependent kinase 5), although no direct phosphorylation of NR2B by Cdk5 has been reported (Hawasli et al., 2007). Cdk5 is a proline-directed serine/threonine kinase that is activated upon interaction with the neuron-specific

cofactors p35 or p39 (Dhavan and Tsai, 2001). Cdk5 has been implicated in numerous CNS processes, including cortical layer formation, neurotransmission, and mnemonic functions (Angelo et al., 2006). Accordingly, a previous study showed that Cdk5 conditional knockout (cKO) mice have improved synaptic plasticity and learning and memory via regulation of NR2B degradation by calpain (Hawasli et al., 2007). Interestingly, transgenic mice overexpressing the truncated Cdk5 activator p25 also exhibit enhanced plasticity and memory formation (Angelo et al., 2003, 2006; Fischer et al., 2005), suggesting that reduced Cdk5 expression or displacement from physiological substrates potentiates synaptic remodeling processes. Despite these results indicating a close mechanistic relationship between NR2B and Cdk5 in the control of mnemonic functions, the underlying molecular processes remain unknown.

Here we show that Cdk5 directly phosphorylates NR2B at Ser1116 and that the phosphorylation state of this serine residue is specifically regulated by physiological neuronal activity. Cdk5-dependent Ser1116 phosphorylation prevents cell surface expression of NR2B-containing NMDAR and thus attenuates synaptic transmission. Disrupting the Cdk5-mediated regulation of NR2B via small interfering peptides (siPs) to block protein-protein interactions reduces this phosphorylation, increases NR2B surface levels, facilitates neurotransmission, and improves hippocampus-dependent learning and memory, suggesting that this regulatory mechanism may indeed be a suitable target for the development of cognitive enhancers.

RESULTS

Cdk5 Phosphorylates NR2B at Ser1116 and Controls Surface Level Expression

Cdk5 has been previously shown to contribute to synaptic plasticity and memory formation through its control of NR2B (GluR2B) levels via calpain-mediated degradation (Hawasli et al., 2007). Because Cdk5 directly associates with this receptor, we investigated whether it could phosphorylate NR2B. To identify novel Cdk5 phosphorylation sites, we employed a PhosphoScan approach utilizing antibody-based enrichment of phospho-peptides from mouse brain with a phospho-specific Cdk5 substrate antibody followed by tandem mass spectrometry (Rush et al., 2005). This approach identified Ser1116 within the cytoplasmic carboxy-terminal of NR2B as a novel Cdk5 phosphorylation site (Figures 1A and 1B). To monitor physiological changes in Ser1116 NR2B phosphorylation, a phosphorylation state-specific antibody was generated. The phospho-Ser1116 (P-S1116) NR2B antibody detected time-dependent in vitro phosphorylation of recombinant NR2B at Ser1116 by Cdk5 (Figure 1C). Analysis of various mouse brain regions, namely cortex, hippocampus, cerebellum, and striatum, further revealed that NR2B is phosphorylated at Ser1116 in vivo (Figures S1A and S1B available online), indicating that this NR2B phosphorylation functions broadly throughout the brain. Treatment of acute mouse hippocampal slices with the specific Cdk5 inhibitor CP681301 caused dose-dependent P-S1116 NR2B reduction (Figure 1D). Moreover, Cdk5 inhibitor-induced reduction of NR2B phosphorylation at Ser1116 followed a similar time course as did the reduction of phospho-Thr75 DARPP-32, a

well-established Cdk5 substrate (Figure S1C; Bibb et al., 1999). Finally, P-S1116 NR2B levels were markedly reduced in hippocampal lysate of Cdk5 cKO mice (Hawasli et al., 2007) compared to wild-type (WT) controls (Figure 1E). Together, these results demonstrate that Ser1116 of NR2B is a physiological Cdk5 phosphorylation site and raise the question of how this post-translational modification might affect NR2B function.

NMDARs are assembled in the endoplasmic reticulum, trafficked along the secretory pathway, and delivered to the postsynaptic plasma membrane (Lau and Zukin, 2007; Wenthold et al., 2003). The molecular machinery underlying NMDAR trafficking and subcellular localization is not yet well characterized, but it has been recognized that phosphorylation of NMDAR subunits including NR2B is important for the regulation of such processes (Chen and Roche, 2007; Ma and Jan, 2002; Wenthold et al., 2003). We noted that Ser1116 of NR2B occurs adjacent to a putative ER retention signal, RXR (Ma and Jan, 2002) (i.e., NH2-…RRRPPRS*PDHK…COOH), and, therefore, investigated whether Cdk5-dependent phosphorylation of NR2B at Ser1116 affected its subcellular localization. The effect of Cdk5 inhibition on NR2B cell surface levels was assessed in cultured hippocampal neurons overexpressing NR2B tagged with extracellular N-terminal green-fluorescent protein (GFP-NR2B). Immunofluorescence staining via anti-GFP antibody thus enabled visualization of cell surface GFP-NR2B. Surface-stained GFP-NR2B exhibited a punctate pattern within dendritic processes (Figure 1F). Counterlabeling with Homer-1, a marker of postsynaptic densities (PSDs), demonstrated that the cell surface fraction of GFP-NR2B localized in proximity to PSDs. Treatment of cultured hippocampal neurons with the Cdk5 inhibitor CP681301 increased surface expression of NR2B in dendritic processes approximately 1.3-fold (Figures 1F and 1G), suggesting that NR2B phosphorylation by Cdk5 modulates NR2B surface levels.

Cdk5-Dependent Regulation of NR2B Function

The abundance of postsynaptic NMDARs is a major determinant of synaptic plasticity and memory formation (Lee and Silva, 2009; Tang et al., 1999). Thus, blocking Cdk5-dependent retention of NR2B from the cell surface could be important in regulating its contribution to NMDAR function. To assess this directly, mouse hippocampal brain slices were treated with either CP681301 or vehicle (Figure 2A). Cdk5 inhibition increased cell surface expression of NR2B 3.5-fold with concomitant reduction in P-S1116 levels to approximately 30% of untreated controls. The effect appeared specific for NR2B because no changes in surface levels of NR2A or the AMPA receptor subunit GluR1 were observed (Figures S2A and S2B).

To evaluate the impact of Cdk5-dependent regulation of NR2B surface levels on physiological function, whole-cell voltage-clamp recording of synaptically evoked NMDAR-mediated excitatory postsynaptic currents (EPSCs) were conducted in CA1 pyramidal neurons of hippocampal slices treated with the Cdk5 inhibitor CP681301 (Figures 2B–2D). Administration of CP681301 increased the NMDAR-EPSC amplitude by approximately 1.5-fold. Furthermore, application of the NR2B-specific inhibitor ifenprodil had a greater attenuating effect on NMDAR-EPSCs in CP681301-treated slices (33% reduction) in comparison to controls (20% reduction) (Figure 2C), suggesting
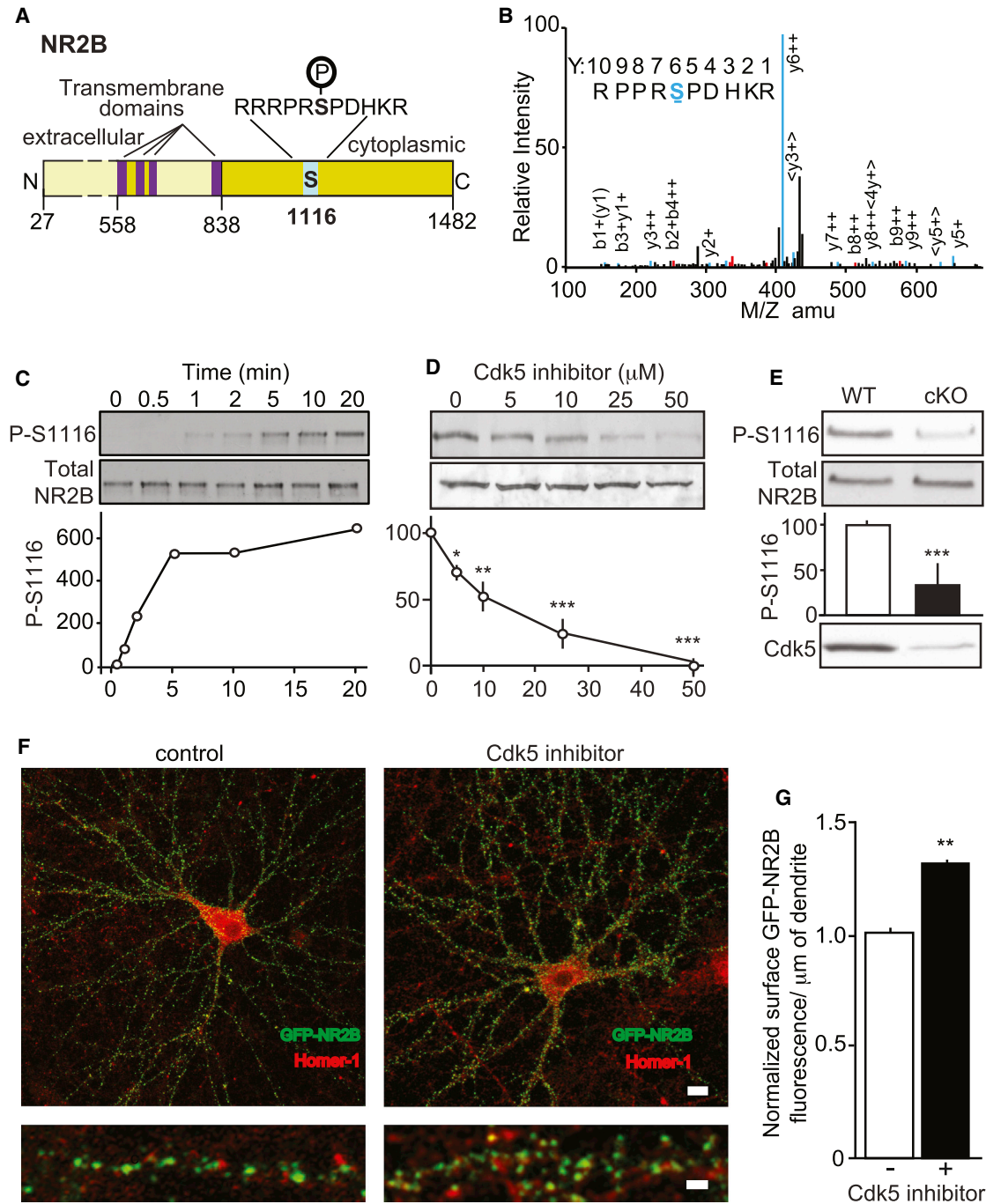
Figure 1. Cdk5 Phosphorylates the NR2B Subunit of the NMDAR at Ser1116 and Regulates Its Cell Surface Expression

(A) Schematic of NR2B indicating domains and motifs.

(B) Positive identification of serine residue 1116 of NR2B as a Cdk5 substrate by LC MS/MS analysis of phospho-peptides immunoprecipitated with phospho-Cdk substrate antibody.

(C) Time-dependent Ser1116 NR2B phosphorylation (P-S1116) by Cdk5 in vitro detected by quantitative immunoblotting. Quantitated values were normalized to total NR2B levels.

(D) Dose-dependent reduction of P-S1116 in hippocampal slices incubated with the Cdk5 inhibitor CP681301 (n = 4; *$p < 0.05$, **$p < 0.01$, ***$p < 0.001$; ANOVA).

(E) Quantitative immunoblot analysis of P-S1116 and total NR2B in hippocampal lysates from Cdk5 cKO and WT mice (n = 4). Loss of Cdk5 in cKO is also shown (bottom).
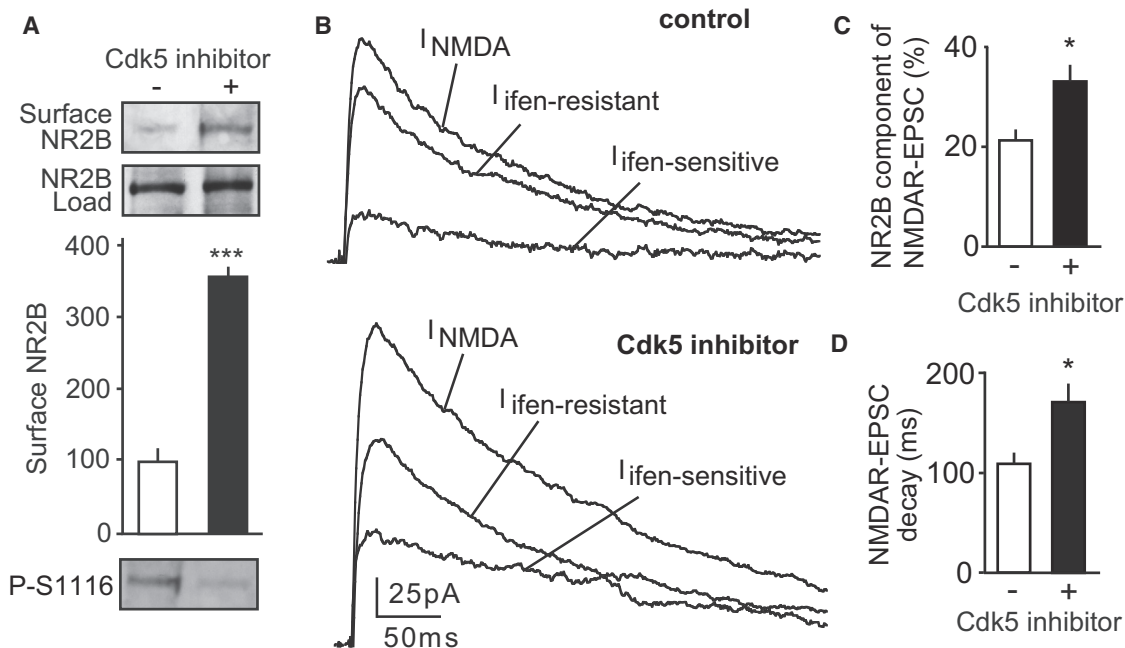
(legend continued on next page)

Figure 2. NR2B Phosphorylation at Ser1116 Regulates NMDAR Function

(A) Increased cell surface NR2B correlates with reduced P-S1116 in hippocampal slices. Levels of cell surface-biotinylated NR2B pulled-down from lysates of hippocampal slices incubated in the absence (-) or presence (+) of the Cdk5 inhibitor CP681301 are shown with blots and quantitation (n = 4). Prior to pull-down, lysates were tested for NR2B Load and P-S1116 (bottom).

(B) Effect of Cdk5 inhibition on the NR2B component of NMDAR-EPSCs. Voltage-clamp EPSC recordings of total NMDAR-EPSCs (I_{NMDA}) in the absence or presence of the specific NR2B inhibitor ifenprodil from pyramidal neurons within the hippocampal area CA1 pretreated with vehicle (control) or the Cdk5 inhibitor CP681301 are shown.

(C and D) Quantitation of NMDAR EPSC recordings showing an increase of ifenprodil-sensitive NR2B component (C) and prolonged decay kinetics (D) of NMDAR EPSCs in cells incubated in the absence (-) or presence (+) of CP681301 (n = 6−7).

Data are represented as mean ± SEM. See also Figures S2A and S2B.

that the NR2B component of NMDAR-EPSCs was increased by Cdk5 inhibition. The deactivation kinetics of NMDAR EPSCs was increased in CP681301-treated slices (170.7 ± 19.4 ms) as compared to untreated slices (112.1 ± 10.5 ms) (Figure 2D). This result is consistent with increased NR2B function in response to CP681301 treatment, because NR2B-containing NMDARs inactivate more slowly than receptors composed of other subunits (Cull-Candy and Leszkiewicz, 2004).

Together, these results indicate that Cdk5 regulates the subcellular localization of NMDAR via NR2B phosphorylation at Ser1116, thereby controlling the level of functional NR2B-containing NMDARs within the synaptic membrane and modulating NMDAR-mediated synaptic currents.

Regulation of Phospho-Ser1116 NR2B by Glutamatergic Neurotransmission, Synaptic Plasticity, and Memory Formation

NMDARs are central to glutamatergic neurotransmission (Bliss and Collingridge, 1993) and are controlled by complex molecular machinery integrating various postsynaptic signaling cascades (Husi et al., 2000; Newpher and Ehlers, 2008). To better understand how Cdk5-dependent NR2B phosphorylation might be regulated and contribute to NR2B function in plasticity and memory formation, the effect of glutamatergic neurotransmission on P-S1116 NR2B was assessed ex vivo and in vivo. Treatment of acute mouse hippocampus slices with NMDA dose-dependently attenuated P-S1116, when normalized to total NR2B levels (Figure 3A). NMDA treatment also reduced total NR2B levels, consistent with previous reports of NMDA-induced, calpain-mediated NR2B degradation (Guttmann et al., 2001; Hawasli et al., 2007). The ability of NMDA to reduce P-S1116 in hippocampal slices was attenuated by treatment with the PP2A/PP1 inhibitor okadaic acid (Figure S2C), indicating that some of the NMDAR-induced effect on P-S1116 is mediated via serine/threonine phosphatase activity.

In agreement with the attenuating effect of NMDA on P-S1116, induction of in vivo long-term potentiation (LTP) in the hippocampal area CA1 also reduced P-S1116. Tetanic stimulation of

(F) Inhibition of Cdk5 increases NR2B cell surface levels in hippocampal neurons. Top panels show immunofluorescence staining of cell surface GFP-NR2B (green) and postsynaptic, intraneuronal Homer-1 (red) in hippocampal neurons treated with vehicle (control) or the Cdk5 inhibitor CP681301. Bottom panels depict high magnification of stained dendrites.

(G) Quantification of cell surface GFP-NR2B fluorescence within dendritic processes (n = 22–26 cells).

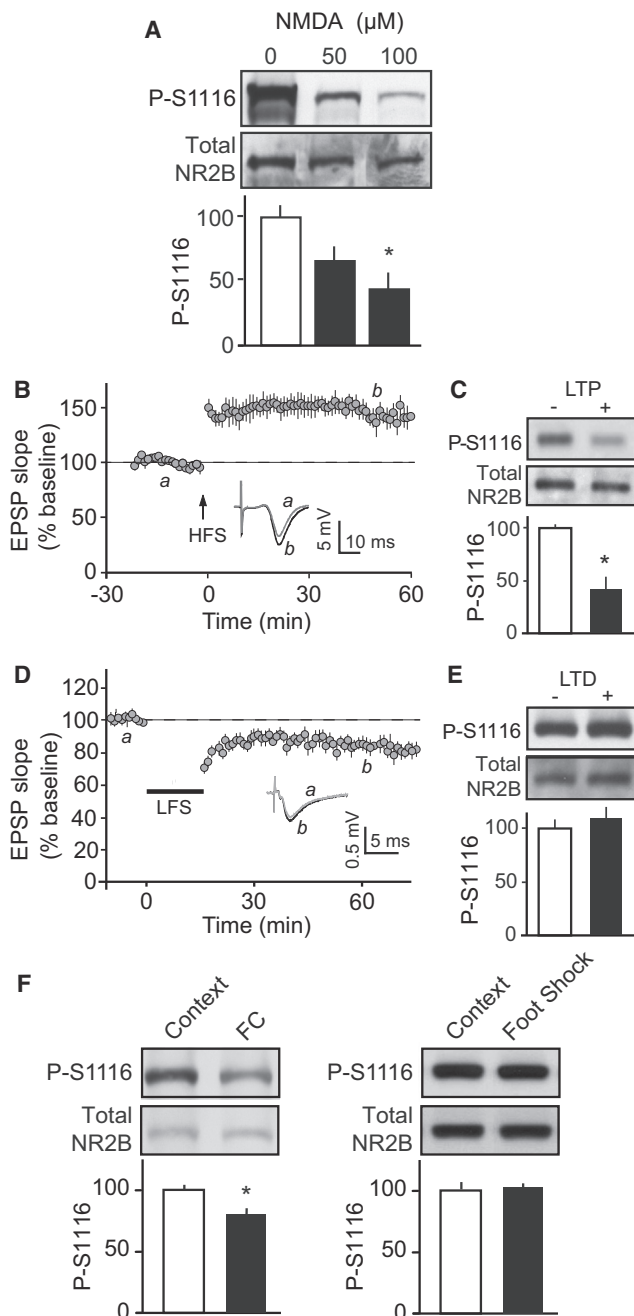Data are represented as mean ± SEM. See also Figure S1.

Figure 3. Phosphorylation of Ser1116 NR2B Is Modulated by Glutamatergic Neurotransmission, Synaptic Plasticity, and Memory Formation

(A) Immunoblots of lysates from NMDA-treated mouse hippocampal slices probed for P-S1116 and total NR2B (n = 4; *p < 0.05; ANOVA).

(B) Induction of in vivo CA1 LTP in mouse. Sample traces of 5 min periods before (a) and after (b) high-frequency stimulation (HFS; two trains of 50 pulses at 100 Hz; 30 s intertrain interval) and LTP induction are shown.

(C) Quantitative immunoblotting of CA1-specific lysates from noninduced (-) and LTP-induced (+) mice for P-S1116 and total NR2B (n = 5).

(D) Induction of CA1 LTD in mouse hippocampal slices with sample traces of 5 min periods before (a) and after (b) low-frequency stimulation (LFS; 900 stimuli at 1 Hz).

mouse Schaffer commissural-CA1 pyramidal cell synapses in vivo caused a significant increase in fEPSP slope (1.4-fold as compared to baseline) that was maintained for 1 hr poststimulus (Figure 3B). One hour after LTP induction, P-S1116 was reduced to approximately 40% of the level in control CA1 lysates (Figure 3C), demonstrating the physiological regulation of P-S1116 in synaptic plasticity. In contrast, induction of long-term depression (LTD) did not affect P-S1116 levels (Figures 3D and 3E). Because excitatory activation of hippocampal NMDAR is integral to learning and memory (Nakazawa et al., 2004), we also assessed the involvement of Cdk5-dependent NR2B phosphorylation in mnemonic processes by evaluating P-S1116 levels after contextual fear conditioning. One hour after training, P-S1116 was reduced in CA1 lysates of fear-conditioned mice to 80% of the levels in nonshocked context-exposed controls (Figure 3F). Foot shock in the absence of context had no effect on P-S1116. Taken together, these results show that NR2B phosphorylation at Ser1116 is regulated by glutamatergic neurotransmission, synaptic plasticity, and learning and memory, suggesting an important role for this signaling mechanism in cognition.

The Protein-Protein Interaction between NR2B and Cdk5 Can Be Selectively Disrupted by Small Interfering Peptides

NR2B and Cdk5 form a complex both in vitro and in vivo (Hawasli et al., 2007). To identify physiological protein-protein interaction sites between NR2B and Cdk5, overlapping eight amino acid peptide cassettes of the NR2B carboxy-terminal domain were synthesized on a peptide microarray microchip (Gao et al., 2004) that was then probed for Cdk5 binding via recombinant Cdk5 followed by immunodetection with anti-Cdk5 antibody (Figure 4A). Four motifs exhibiting high Cdk5 binding were identified by this approach (Figure 4B). To determine whether these motifs were actual NR2B-Cdk5 interaction sites, peptides corresponding to these motifs were synthesized and tested for their ability to interfere with NR2B-Cdk5 binding. In this screen, the peptide corresponding to amino acid residues 1111–1127 (RRPPRSPDHKRYFRDKE; NR2B small interfering peptide [NR2B siP]) most potently blocked the pull-down of Cdk5 by recombinant GST-tagged NR2B in vitro (Figure 4C). Moreover, the NR2B siP dose-dependently inhibited in vitro phosphorylation of Ser1116 NR2B by Cdk5 (Figure 4D). In contrast, a scrambled control peptide (RRRSYFHKEDRPPRDK) did not attenuate Ser1116 phosphorylation in vitro. Interestingly, the NR2B siP did not inhibit the in vitro phosphorylation of inhibitor-1 (Figure S3A), a well-defined Cdk5 substrate (Nguyen et al., 2007), indicating that the inhibition of Ser1116 NR2B phosphorylation by NR2B siP was specific.

To further assess the efficacy and consequences of targeting Cdk5-NR2B protein interactions by small interfering peptides ex vivo and in vivo, cell-permeabilizing polyarginine or penetratin

(E) Quantitative immunoblotting of noninduced (-) and LTD-induced (+) CA1-specific lysates probed for P-S1116 and total NR2B (n = 5).

(F) Quantitative immunoblots of CA1-specific lysates from contextual fear conditioned (FC) and control (Context and Foot Shock) mice obtained 1 hr after training for P-S1116 and total NR2B levels (n = 4–6).

Data are represented as mean ± SEM. See also Figure S2C.

N-terminal tags were included in the NR2B siP and control peptides. These tags are commonly used to deliver peptides across the cell membrane into the cytosol of neurons (Joliot and Prochiantz, 2004).

Consistent with the effects observed in vitro, application of the NR2B siP to hippocampal slices decreased P-S1116 in a time- and dose-dependent manner (Figures 4E and S3B). Treatment with the NR2B siP did not alter levels of NR2B or Cdk5 expression (Figures 4E and S3B). The specificity of NR2B siP observed in vitro was retained in vivo; it had no effect on the phosphorylation state of the well-characterized Cdk5 site Thr75 DARPP-32 (Bibb et al., 1999), but it time-dependently reduced P-S1116 in acute mouse striatal slices (Figures S3C and S3D). These data show selective modulation of P-S1116 by siP and also that this mechanism may be targeted in multiple limbic structures mediating learning and memory. Furthermore, NR2B siP treatment of hippocampal slices effectively blocked subsequent coimmunoprecipitation of Cdk5 and NR2B (Figure 4F), indicating that siP disrupts Cdk5-NR2B protein-protein interactions. In contrast, treatment with scrambled control or the Cdk5 inhibitor CP681301 did not affect Cdk5-NR2B interactions.

Consistent with our data that Cdk5 regulates NR2B cell surface expression, the siP induced a 3.3-fold increase in NR2B cell surface levels in hippocampal slices (Figure 4G). Finally, cell surface GFP-NR2B levels increased 1.5-fold after 30 min treatment with NR2B siP as compared to control peptide (S1116A) in primary hippocampal cultures (Figures 4H and 4I). Thus, Cdk5-NR2B protein-protein interactions can be targeted in intact brain tissue with NR2B siP, resulting in reduced Cdk5-dependent phosphorylation of Ser1116 NR2B and appreciable increases in cell surface expression of the receptor.

Disruption of NR2B-Cdk5 Interaction by NR2B siP Increases NR2B Function and Facilitates Synaptic Transmission

Given the efficacy of the NR2B siP in targeting Cdk5-NR2B interactions and increasing NR2B cell surface levels, its impact on NMDAR-mediated EPSCs was assessed. Treatment of cortical slices with the NR2B siP produced a 1.8-fold increase in the NMDA/AMPA EPSC ratio as compared to a scrambled control peptide (Figure 5A). Moreover, slices incubated with NR2B siP exhibited a 1.5-fold increase in the ifenprodil-sensitive NR2B component of NMDAR EPSCs (Figures 5B and 5C), suggesting that the NR2B siP-induced increase in NMDAR EPSCs is due to recruitment of additional NR2B-containing NMDAR to the cell surface.

Given the importance of NR2B in mediating the potentiation of synaptic transmission during plasticity, we assessed the effects of NR2B siP on extracellularly recorded field excitatory postsynaptic potentials (fEPSP) in the hippocampal CA3-CA1 pathway. Treatment of hippocampal slices with NR2B siP rapidly induced a 1.9-fold increase in fEPSP slope compared to slices infused with a control peptide (Figures 5D and 5E). Upon washout of the NR2B siP, fEPSP slopes progressively decreased until they reached steady-state levels with fEPSP slopes that were 1.6-fold greater than control treated slices.

To determine whether the NR2B siP-induced changes in hippocampal neurotransmission were due to NR2B, the effects of

the NR2B siP on basal fEPSPs were assessed in slices coincubated with the specific NR2B antagonist Ro25-6981 (Figures 5F and 5G). Under these conditions, the NR2B siP-mediated increase was blocked. Cdk5 cKO mice lack approximately 70% of hippocampal Cdk5 and exhibit a reduced threshold for induction of LTP but have normal baselines for fEPSP fiber volley amplitude (Hawasli et al., 2007). Interestingly, the ability of the NR2B siP to raise CA1-CA3 fEPSPs was almost absent in Cdk5 cKO mice with a small (1.2-fold) but still significant increase in fEPSP slopes (Figures 5F and 5G). Thus the effect of the peptide on synaptic transmission is mediated via NR2B and Cdk5. Together these results show that NR2B siP selectively disrupts NR2B-Cdk5 interaction, reduces P-S1116, increases cell surface levels of NR2B, and facilitates neurotransmission by enhancing NR2B function.

NR2B siP Improves Learning and Memory

The data presented so far indicate that the subcellular localization of NR2B is regulated by Cdk5. Reduction in Cdk5 activity, as well as disruption of Cdk5-NR2B interaction, consistently increased NR2B surface levels and facilitated NMDA-mediated synaptic function. Because previous research has demonstrated that elevated NR2B function enhances cognitive performance (Lee and Silva, 2009; Tang et al., 1999), we investigated whether administration of NR2B siP can improve mnemonic function. For this purpose, we first established robust in vivo protocols to deliver cell-penetrating NR2B siP to the appropriate brain regions and test their effect on learning and memory. NMDARs are required for hippocampus-dependent learning and memory, such as acquisition of contextual fear memory (Barkus et al., 2010; Bast et al., 2003). Accordingly, infusion of the selective NR2B inhibitors Ro25-6981 or ifenprodil into dorsal hippocampus was previously found to impair contextual fear learning, but not locomotor or anxiety-related behavior (Zhang et al., 2008). Hence, NR2B siP was infused bilaterally into the CA1 subfield of dorsal hippocampus continuously for 72 hr via mini-osmotic pumps. Because of the size of the osmotic pump and the robust behavioral performance, these initial experiments were performed in rat. Spatiotemporal tracking of fluorescein-tagged NR2B siP (FITC siP) confirmed correct targeting, continuity of the delivery, and neuronal uptake of the peptide. FITC siP was specifically detected in dorsal hippocampus at 12, 24, and 72 hr after initiation of pumping. The FITC siP was present in hippocampal area CA1 and labeled the cytoplasm of pyramidal neurons (Figure 6A). After pumping was stopped, intracellular FITC siP signal was markedly reduced by 6 hr and had largely disappeared by 24 hr (Figure S4A).

Within the FITC siP-infused region, P-S1116 was reduced by approximately 40% compared to FITC scrambled peptide-infused controls (Figure 6B). Infusion of FITC siP also caused a 3-fold increase in NR2B surface expression (Figure 6C). Together, these results validate this approach for the delivery of NR2B siP into pyramidal neurons of dorsal hippocampus and show that the NR2B siP induces biochemical and cellular changes in vivo comparable to our in vitro and ex vivo observations.

With these parameters established, the effect of NR2B siP infusion on fear memory was evaluated. Continuous bilateral NR2B siP infusion into rat dorsal hippocampus 24 hr prior to fear
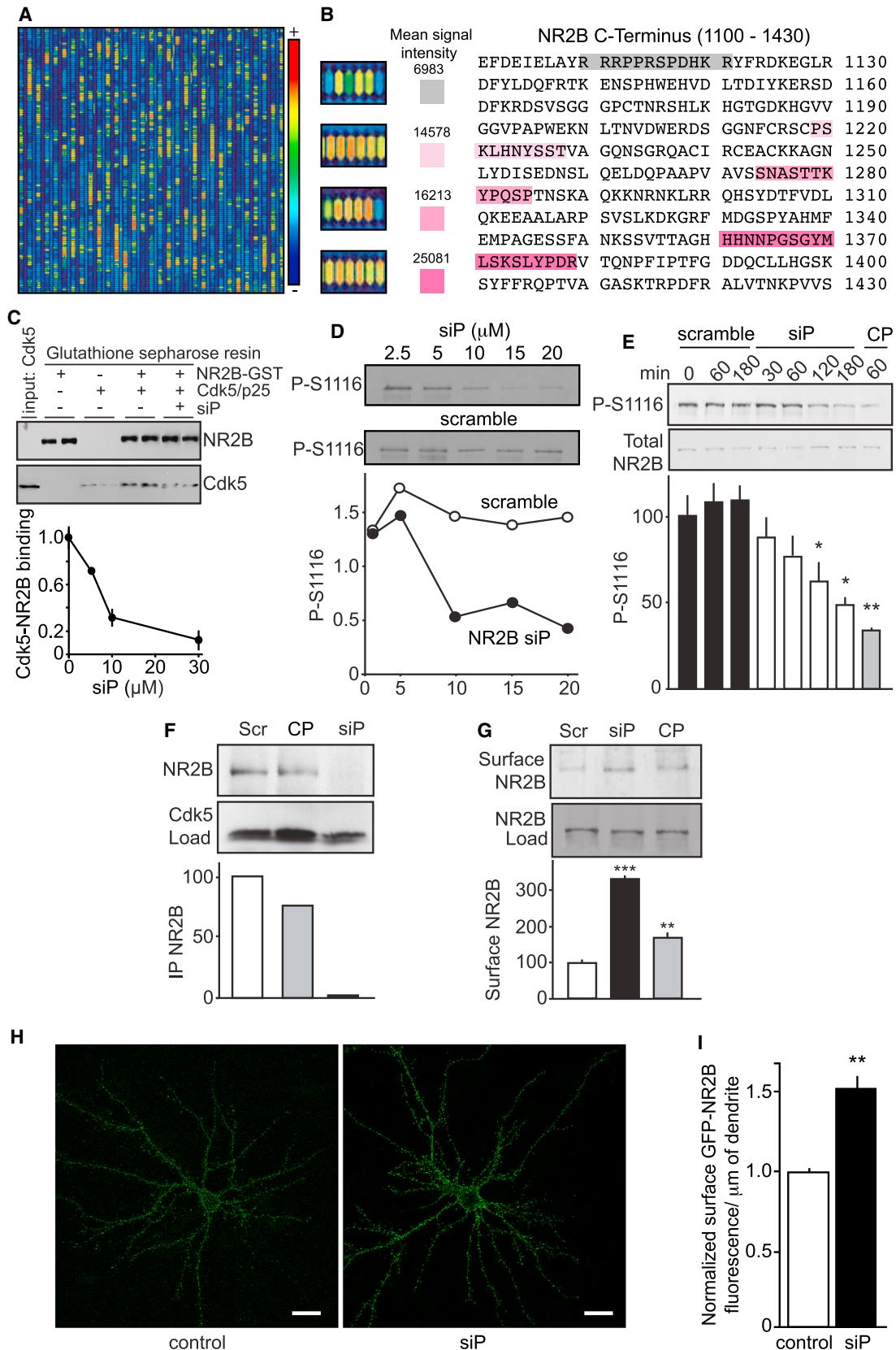
(legend on next page)

conditioning increased hippocampus-dependent contextual fear memory 1.7-fold compared to scrambled peptide controls (Figure 6D). In agreement with the hippocampal-independent nature of cue-associated fear learning (Phillips and LeDoux, 1992), no effect was observed on tone-induced freezing. Administration of neither NR2B siP nor scrambled control affected nociception, pain threshold, or motor reflexes (Figures S4B and S4C). During extinction trials, contextual memory enhancement persisted in NR2B siP-treated rats at 48 and 72 hr after initial training (Figure S4D and S4E). The conditioned fear response was extinguished by 96 hr for both groups (Figure S4E). After extinction and expiration of the mini-osmotic pump, rats were retrained. Twenty-four hours after retraining, the contextual fear memory was increased in rats previously infused with NR2B siP during the initial acquisition phase, but not scrambled controls (Figure S4F), suggesting that behavioral effects persist even after NR2B siP clearance. These data also indicate that the siP-improved memory may have been more retained or consolidated.

The learning and memory improvements associated with NR2B siP infusion correlated directly with reduced P-S1116 NR2B. NR2B siP infusion and fear conditioning both decreased P-S1116 NR2B in CA1 1 hr after training (Figure S5A). Animals that had been infused with NR2B siP and undergone fear conditioning exhibited the lowest phosho-Ser1116 levels.

Previous studies found that NMDAR inhibition during the acquisition phase impaired fear memory (Bast et al., 2003; Zhang et al., 2008; Zhao et al., 2005). Therefore, we evaluated whether an acute NR2B siP infusion shortly before the training session could also improve fear memory. For this purpose, 3-month-old mice were acutely surgerized under isofluorane anesthesia and NR2B siP was infused into dorsal hippocampus 90 min prior to fear conditioning. Acute NR2B siP infusion resulted in significantly elevated freezing behavior in the context test as compared to controls (Figure 6E). The freezing levels during the context test of the acute paradigm were, in fact, comparable to the levels observed with chronic infusion. The tone test did not reveal any significant changes between acute peptide-infused groups. Finally, to evaluate whether NR2B siP administration may be a valid treatment for age-related cognitive decline, 14-month-old mice were acutely infused with NR2B siP and tested for fear memory (Figure S5B). As observed for

3-month-old mice, acute NR2B siP infusion 90 min prior to training increased contextual fear memory 1.7-fold compared to control peptide or noninfused cannulated controls. Thus, increasing NR2B surface levels may be a suitable memory enhancement strategy even for later stages in life. These results are also consistent with studies showing that NR2B overexpression in forebrain neurons improves learning and memory in aged mice (Brim et al., 2013; Cao et al., 2007).

Taken together, these findings show that selective disruption of NR2B-Cdk5 interactions via NR2B siP enhances hippocampus-dependent learning and memory through potentiation of a regulatory mechanism that is involved in memory formation. Thus, it is possible that this mechanism regulating NR2B function via Cdk5 may be a suitable target for the development of cognitive enhancers as therapeutics for memory impairment as well as age-dependent cognitive decline.

DISCUSSION

In this study, we present a molecular mechanism regulating the subcellular localization of NR2B-containing NMDAR. This mechanism appears to be central to synaptic transmission and mnemonic functions and can be targeted to enhance memory. A model of this mechanism and the effects of targeting it may be suggested (Figure 6F). Upon glutamatergic neurotransmission, such as that occurring during synaptic plasticity induction or memory formation, Cdk5-dependent Ser1116 phosphorylation is reduced and subsequently leads to increased cell surface levels of NR2B-containing NMDAR. Consequently, selective disruption of NR2B-Cdk5 interactions via the NR2B siP increases NR2B surface levels, thereby facilitating synaptic transmission. Intrahippocampal infusion of the NR2B siP improved fear memory, suggesting that the regulation of NR2B by Cdk5 may be a suitable target for the development of cognitive enhancers.

The molecular basis of cognition is thought to involve activity-dependent changes in intracellular signaling, gene expression, protein synthesis, remodeling of synapses, and neurotransmission (Bibb et al., 2010). In particular, excitatory glutamatergic neurotransmission, as well as its regulatory machinery and downstream targets, have been singled out as central molecular

Figure 4. Identification of NR2B-Cdk5 Interaction Motifs and Development of a Small Interfering Peptide

(A) Peptide microarray of the NR2B C-terminal domain showing high (+, red) to low (-, blue) Cdk5 binding regions.

(B) The cytoplasmic C terminus amino acid sequence of NR2B with potential Cdk5 binding sites highlighted with their corresponding peptide array tiles.

(C) NR2B siP blocks pull-down of Cdk5 with recombinant NR2B immobilized on GST beads, demonstrating disruption of NR2B-Cdk5 interaction in vitro. Immunoblots show relative levels of NR2B and Cdk5 under conditions indicated. NR2B siP dose dependently disrupts NR2B-Cdk5 binding in vitro as depicted in plot (n = 3).

(D) Immunoblots showing that NR2B siP dose dependently inhibits in vitro phosphorylation of Ser1116 NR2B by Cdk5, whereas the control peptide (scramble) has no effect.

(E) Time-dependent reduction of P-S1116 in hippocampal slices treated with NR2B siP (25 μM) or the Cdk5 inhibitor CP681301 (CP; 50 μM), but not scrambled (Scr) control peptide (n = 4; *p < 0.05, **p < 0.01; ANOVA).

(F) NR2B siP, but not the scrambled peptide, nor CP681301 (CP) disrupts NR2B-Cdk5 interaction in hippocampal slices (four pooled slices for each sample) as evaluated by coimmunoprecipitation. Cdk5 Load is also shown.

(G) NR2B cell surface levels are increased in hippocampal slices treated with NR2B siP (1 hr, 100 μM) or the Cdk5 inhibitor CP681301 (1 hr, 50 μM), but not with control peptide (Scramble; 1 hr, 100 μM) (n = 4; **p < 0.01; ***p < 0.001; ANOVA). NR2B Load is also indicated.

(H) Immunofluorescence staining of cultured hippocampal neurons for surface GFP-NR2B after treatment with control peptide or NR2B-siP.

(I) Quantification of dendritic cell surface GFP-NR2B (n = 49–64 cells).

Scale bars represent 20 μm. Data are represented as mean ± SEM. See also Figure S3.
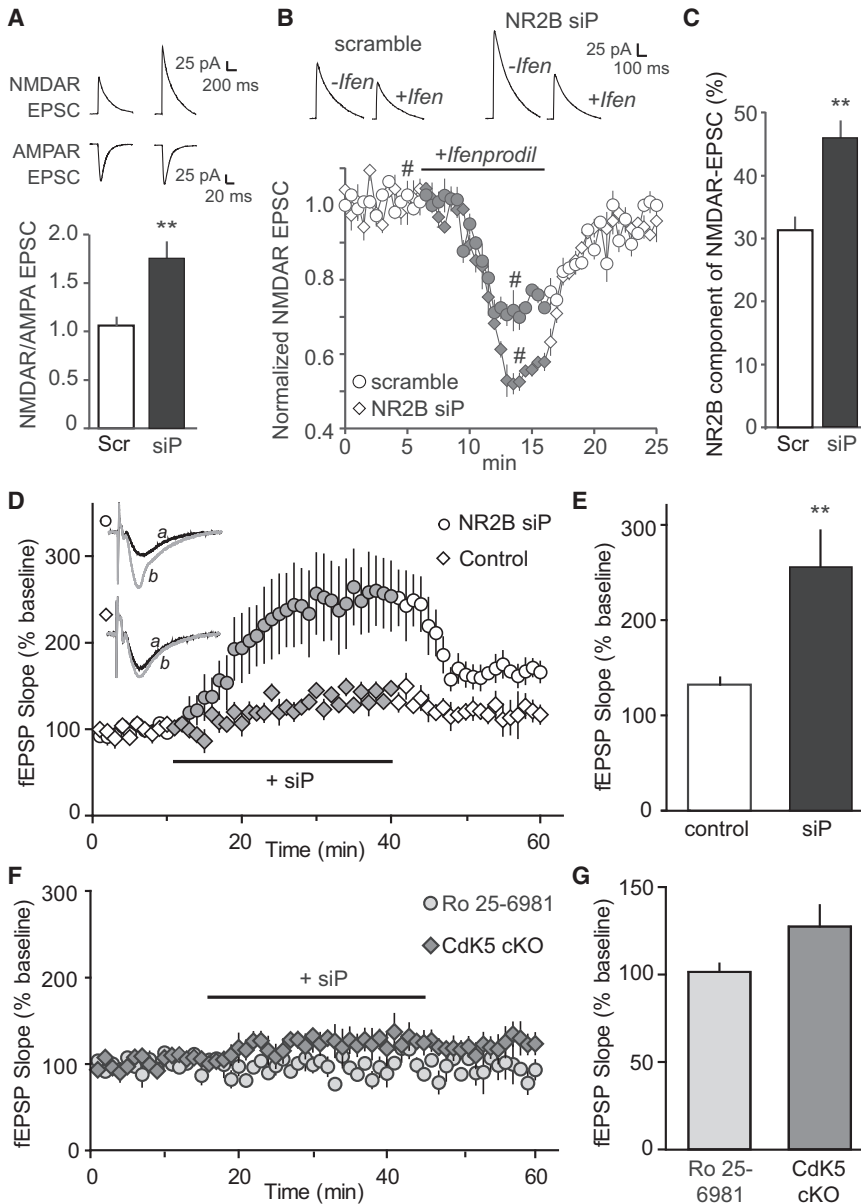
Figure 5. Disruption of NR2B-Cdk5 Interaction by NR2B siP Facilitates Synaptic Transmission

(A) Recordings and quantification of NMDAR/AMPAR EPSC ratio from cortical pyramidal neurons treated with NR2B siP or scrambled (Scr) control (n = 12–16).

(B and C) NMDAR EPSC sensitivity to the NR2B inhibitor, ifenprodil, in slices incubated with NR2B siP or scrambled control (n = 6–7).

(D and E) Extracellular CA3-CA1 field recordings in hippocampal slices treated with NR2B siP or control peptide (30 min, 2 μM). Sample traces of 2 min before (a) and at end (b) of siP application and Quantitation of fEPSP slope (n = 4).

(F and G) Extracellular field recordings in hippocampal slices incubated with the specific NR2B inhibitor Ro 25-6981 (3 μM) or from Cdk5 cKO were treated with NR2B siP (30 min, 2 μM) and quantification of fEPSP slope (n = 3) did not show a significant effect of NR2B siP with NR2B inhibition or in absence of Cdk5 (cKO).

Data are represented as mean ± SEM.

to the postsynaptic density and may prevent endocytosis. Furthermore, NR2B has been suggested to traffic dynamically from extra- to intrasynaptic locations on the cell surface, possibly through association of its extreme C terminus with different members of the membrane-associated guanylate kinase (MAGUK) family. In contrast, Ser1116 appears to reside within a region of the cytoplasmic terminus that interacts with early components of receptor trafficking in the postsynaptic endoplasmic reticulum (Vandenberghe and Bredt, 2004).

Previously, Cdk5 cKO was shown to increase total NR2B levels by disrupting the NR2B-Cdk5-calpain complex, thereby attenuating activity-dependent degradation of NR2B by calpain (Hawasli et al., 2007). Here, pharmacological inhibition of Cdk5 revealed that the protein kinase also phosphorylates NR2B, thereby modulating the activity-dependent trafficking of the receptor to the cell surface. Thus, Cdk5 appears to have two roles, regulating NR2B trafficking as well as metabolism. Both these roles are probably important for synaptic plasticity and memory, although the temporal sequence and molecular integration of these two activity-dependent events requires further study.

It also remains to be determined whether dephosphorylation of Ser1116 targets NR2B selectively to the synapse or to both synaptic and extrasynaptic compartments. As the increases in cell surface NR2B observed here were greater than the potentiation of NR2B-mediated current, it is possible that not all NR2B driven to the surface was functional. Interestingly, other NMDAR subunits possess endoplasmic reticulum retention motifs similar

mechanisms. Signaling cascades that modulate expression, activity, trafficking, and degradation of neurotransmitter receptors are critical to the formation of memories (Chen and Roche, 2007; Lau and Zukin, 2007; Wenthold et al., 2003). Accordingly, enhanced synaptic plasticity, learning, and memory has been observed in several animal models that feature increased NR2B surface levels as a result of manipulating various molecular processes including NR2B expression, trafficking, and degradation (Crair and Malenka, 1995; Hawasli et al., 2007; Lee and Silva, 2009; Tang et al., 1999; Wong et al., 2002; Yin et al., 2011). Thus, a robust body of data singles out NR2B as a prominent factor for cognitive function.

NR2B has been shown to serve as a substrate of various protein kinases (Wenthold et al., 2003). In particular, tyrosine phosphorylation of its extreme C terminus modulates its anchoring

to the one indicated here in NR2B. Furthermore, some of these are also regulated via phosphorylation (Scott et al., 2001) and in response to neuronal activity (Mu et al., 2003), suggesting a common overall process in synaptic remodeling or homeostasis.

Numerous neurodevelopmental, neurological, and neuropsychiatric disorders, such as Alzheimer's disease, depression, and schizophrenia, manifest cognitive deficits. Interestingly, deficiencies in NMDAR trafficking have been implicated in the pathophysiology of many of these diseases (e.g., see Snyder et al., 2005). Moreover, age-related cognitive decline occurs progressively in all aging humans, albeit at variable rates. Although behavioral interventions are being advanced as one group of approaches, effective treatments to counter cognitive deficits or memory decline are extremely limited.

Peptides are now an integral component of CNS research, and protein-protein interactions and intracellular signaling mechanisms provide a very large base of new therapeutic targets (Jubb et al., 2012). Until recently, CNS drug discovery has focused on developing synthetic small molecules that act primarily upon targets involved in neurotransmission including receptors and ion channels. Drug target pool algorithms such as the "rule of five" (Lipinski, 2000) and "the druggable genome" (Hopkins and Groom, 2002) have been used in an effort to facilitate the discovery of small molecules of high specificity for oral delivery. However, these restrictions have often had the unintended consequences of producing molecules with poor selectivity and unwanted side effects. Larger molecules including peptides and peptidomemetics that interfere with protein-protein interactions provide more contact with targets and greater selectivity but have been limited by low bioavailability, poor membrane permeability, and metabolic instability. These obstacles are being circumvented by a number of creative means and protein- or peptide-based drugs are now roughly 10% of the pharmaceutical market and growing (Craik et al., 2013). As an example of this potential, peptides that target NR2B interactions with the postsynaptic density have been shown to neuroprotect from ischemic injury in primates (Cook et al., 2012).

Here we demonstrate memory enhancement by selectively targeting a single phosphorylation site and NR2B-Cdk5 protein-protein interactions with a peptide injected intracranially. It will be interesting to find out whether further optimization in the targeting of this and other synaptic mechanisms will lead to more practical delivery modes and clinically applicable therapies.

EXPERIMENTAL PROCEDURES

Please see the Supplemental Experimental Procedures for detailed methods on phosphorylation-site identification, phosphorylation state-specific antibody generation, in vitro phosphorylation, binding assays, peptide array analysis, in vivo LTP, whole-cell recordings, hippocampal cannulation, and siP infusion.

Antibodies and Reagents

Cdk5 (C-8) and NR2A antibodies (Ab) were obtained from Santa Cruz; P-Thr75 DARPP-32, DARPP-32, and Inhibitor-1 Ab were from Cell Signaling Technology; EGFP, FITC, and α-tubulin Ab were from Abcam; NR2B Ab was from PhosphoSolutions; Homer-1 Ab was from Synaptic System; MAP-2 and NeuN Ab were from Millipore; secondary anti-mouse, anti-rabbit, and anti-goat IgG Ab were from Pierce; Cy3-conjugated anti-rabbit IgG secondary Ab was from Jackson Immunoresearch; and Alexa 647-conjugated anti-

mouse IgG secondary Ab was from Molecular Probes. P-Ser6 inhibitor-1 Ab was previously described (Nguyen et al., 2007). The specific Cdk5 inhibitor CP681301 was provided by Pfizer Pharmaceutical. Ifenprodil and Ro 25-6981 were from Tocris. All peptides were synthesized by the UT Southwestern Protein Chemistry Technology Center utilizing the Perseptive Biosystems Pioneer and Applied Biosystems 433 synthesizers. Peptides were verified by mass spectrometry analysis and reversed-phase HPLC chromatography. The sequences of the small interfering peptides (siP) were NR2B siP, RRPPRSPDHKRYFRDKE; scrambled, RRRSYFHKEDRPPRDK; R7 NR2B siP, RRRRRRRRPPRSPDHKRYFRDKE; R7 scrambled, RRRR RRRRRSYFHKEDRPPRDK; Pen NR2B siP, RQIKIWFQNRRMKWKK-PPRS PDHKRYFRDKE; and Pen control, RQIKIWFQNRRMKWKK-PPR**A**PDHK RYFRDKE. The FITC tag was attached at the C terminus of the siP.

Animals

Animals were housed in a 12 hr light/dark cycle (lights on from 6:00 a.m. to 6:00 p.m.), with food and water available ad libitum. Mice in the C57BL/6 background were obtained from Jackson and were housed 3–4 per cage. Cdk5 cKO mice were bred and maintained as previously specified (Hawasli et al., 2007). For all experiments, age-matched male littermates were used, unless otherwise noted. Sprague-Dawley rats were obtained from Charles River Laboratories and bred and maintained at the UT Southwestern animal facility. All behavioral experiments were conducted in the UTSW Rodent Behavior Core. All experimental procedures were reviewed and approved by the University of Texas Southwestern Institutional Animal Care and Use Committee (IACUC).

### Slice Pharmacology, Immunoprecipitation, and Cell Surface Labeling

Hippocampal, striatal, and cortical slices were prepared as previously described (Hawasli et al., 2007; Sahin et al., 2006; Yuen et al., 2012). Pharmacological treatments were performed in Mg^{2+}-free Kreb's buffer containing NMDA (50 or 100 μM, 15 min), CP-681301 (5–100 μM, 60 min), or siP (0–100 μM, 0–180 min). The R7-tagged peptides were used in slice experiments assessing substrate phosphorylation levels. Cell surface biotinylation assays were performed with Pierce Cell Surface Protein Isolation Kit (Thermo Scientific) according to manufacturer's instructions. In brief, hippocampal slices were equilibrated in ice-cold oxygenated ACSF for 5 min and then incubated for 30 min in ACSF with Sulfo-NHS-SS-Biotin (0.5 mg/ml in ACSF; Pierce). Biotinylation reaction was quenched with ACSF containing 50 mM NH_4Cl and 50 mM glycine and tissue was dissected in ice-cold dissection buffer containing protease and phosphatase inhibitors (Plattner et al., 2006). Immunoprecipitation (IP) was performed as previously described (Plattner et al., 2006).

Lysate Preparation and Immunoblotting

Brain dissection, tissue removal, and lysate preparation were performed with specific emphasis on maintaining protein integrity and phosphorylation levels by using protease and phosphatase inhibitors as described (Bibb et al., 1999; Plattner et al., 2006). Graphs of all quantitative immunoblot analyses of P-S1116 NR2B represent the ratio of P-S1116/total NR2B. Hippocampal subfield CA1 tissue including stratum radiatum, stratum pyramidale, and stratum oriens was microdissected in ice-cold dissection buffer containing protease and phosphatase inhibitors (Plattner et al., 2006) via a dissecting microscope. After excision of the intact hippocampus from the brain, the dentate gyrus and CA3 were removed longitudinally with the basal vein and the hippocampal fissure as guidance clues.

Extracellular Field Recordings

Hippocampal slices were prepared from 3-month-old C57BL/6 mice as described (Hawasli et al., 2007) and field excitatory postsynaptic potentials (fEPSP) from CA1 were evoked by square current pulses (0.1 ms at 0.033 Hz) with a bipolar stimulation electrode placed at the Schaffer collaterals. Results were obtained with a stimulus intensity to induce 50% of the maximal fEPSP slope. Once the baseline was stable, Pen siP or Pen control peptides were added to the perfusion buffer for 30 min. For recordings performed in the presence of the NR2B selective blocker Ro 25-6981, the Pen siP peptide was added 10 min after starting Ro 25-6981 (3 μM) bath perfusion.
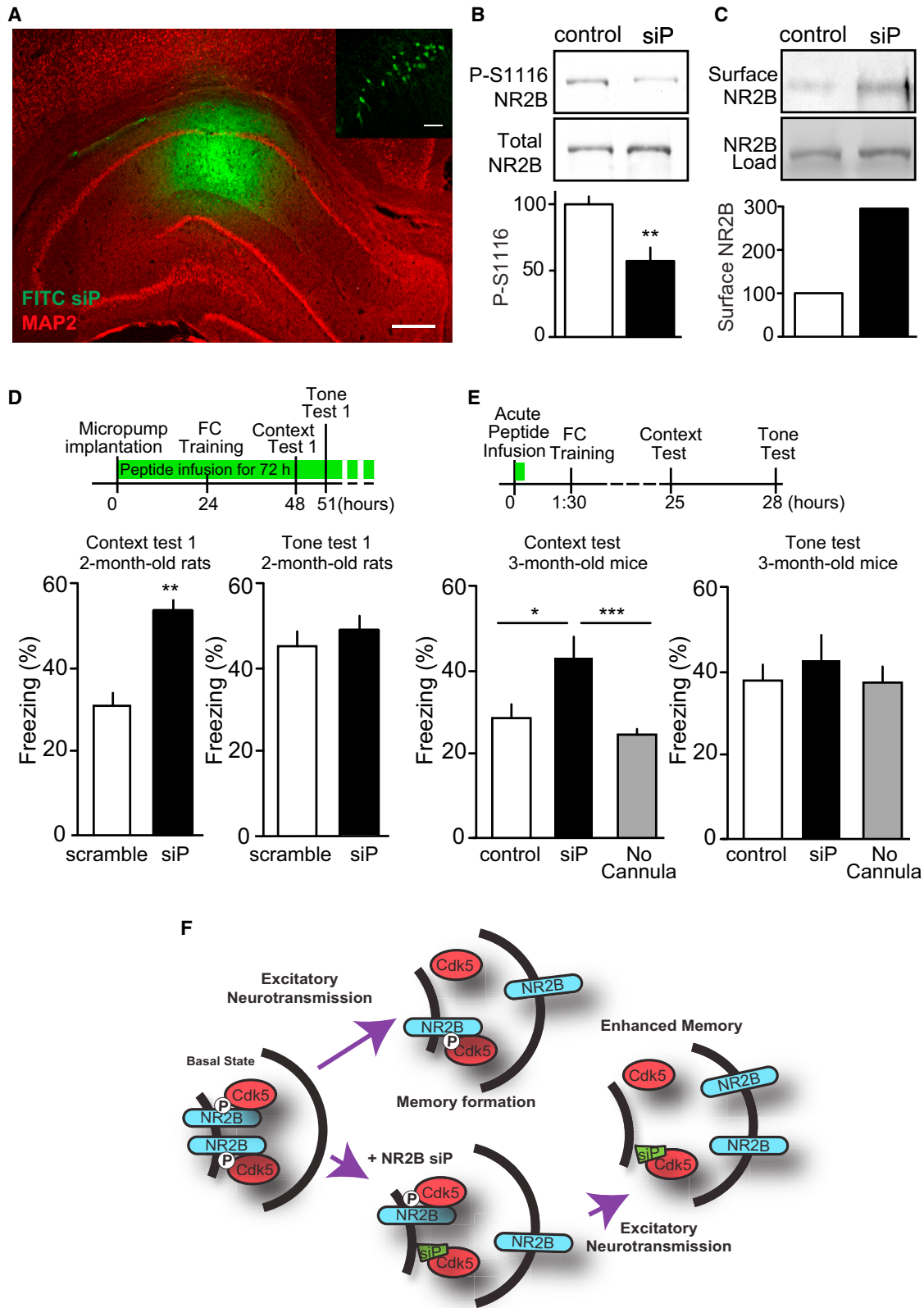
The effects of the siPs were evaluated as percent change from baseline fEPSP slope.

LTD analysis was performed in hippocampal slices from 16- to 17-day-old C57BL/6 mice as previously reported (Billard, 2010; Milner et al., 2004) via modified ACSF (in mM: 130 NaCl, 26 NaHCO₃, 3 KCl, 1 MgCl₂, 1.25 NaH₂PO₄, 2 CaCl₂, 10 glucose [pH 7.4], 300 mOsm). After 15 min of stable baseline recording, a low-frequency stimulation protocol (900 stimuli at 1 Hz) was applied to induce LTD that was maintained for at least 1 hr. At the end of the LTD recording, the CA1 was microdissected and homogenized in lysate buffer containing protease and phosphatase inhibitors.

Dissociated Neuronal Cultures, Transfection, Drug Treatments, and Live-Labeling of Cell Surface Receptors

Dissociated hippocampal neurons were prepared from P0 rats as described in Goda and Colicos (2006) and plated onto glass coverslips coated with poly-D-lysine (10 μg/ml) and laminin (2 μg/ml). Cultures were maintained in Neurobasal media (Invitrogen) supplemented with 6 mg/ml glucose, 0.1% Mito serum extender, 2.5% B27, and 2 mM Glutamax. Hippocampal neurons were transfected at DIV 7–8 by the calcium-phosphate method and used at DIV 14–18. Constructs include pRK5-EGFP-NR2B that encodes a N-terminally EGFP-tagged NR2B subunit (GFP-NR2B).

To evaluate the effect of Cdk5 inhibition on cell surface expression of NR2B, neuronal cultures were treated with 25 μM CP68130 for 1 hr or with 2 μM NR2B-siP for 30 min, 6–10 days after transfection with pRK5-EGFP-NR2B. DMSO or control peptides were used as controls. Immunofluorescence staining of cell surface GFP-NR2B was performed by incubating nonpermeabilized, live neuronal cultures with rabbit polyclonal EGFP ab (1:500, Abcam, Ab6556) for 15 min at 37°C (Cingolani et al., 2008; Pozo et al., 2012). Neurons were fixed in PBS containing 4% paraformaldehyde and 4% sucrose for 10 min at 25°C and then permeabilized and blocked with PBS containing 10% fetal bovine serum, 0.2% gelatine, and 0.02% Triton X-100 for 1 hr at 25°C. After incubation with mouse monoclonal Homer-1 ab (1:1,000, SYSY, 160011) for 1 hr at 25°C, neurons were washed and incubated with Cy3-conjugated anti-rabbit IgG and Alexa 647-conjugated anti-mouse IgG for 1 hr at 25°C. Cells were washed and mounted onto microscope slides for confocal imaging. Z-stacks were acquired with an inverted 510 Meta Zeiss confocal microscope with a 63× water objective, sequential mode, and 4 frames average. Baseline microscopy settings were established for control cultures and maintained constant throughout the entire imaging session. ImageJ was used to project Z-stacks and measure dendritic fluorescence. Dendritic length was assessed by tracing processes with NeuronJ and used to normalize dendritic fluorescence.

Animal Behavior

All behavior was carried out with the experimenter blind to treatment groups. For cued fear conditioning in rats, animals were left to explore the conditioning box (Med Associates) for 2 min, followed by a 30 s period with tone representation (90 dB, 10 kHz), which coterminated with a mild foot shock (2 s, 0.7 mA, constant current). Rats remained in the chamber 2 min after shocking before returning to their home cage. Conditioning boxes were thoroughly cleaned after each animal. To test context-dependent fear memory, rats were reintro-duced 24 hr after shock into the conditioning box for 5 min. Freezing responses (motionless except respirations) were recorded via a 5 s interval time-sampling method. Twenty-seven hours after conditioning, tone-recall was assessed in a novel context with novel odor (vanilla). The rats were left exploring the novel context for 3 min without tone followed by a 3 min period with tone representation. Extinction of fear memory was evaluated by re-exposing rats to the conditioning box at 24, 48, 72, and 96 hr after shock for 5 min. After fear memory extinction, rats were retrained with a 0.7 mA foot shock, and contextual learning was analyzed 24 hr after retraining. Nociceptive response and motor reflex were evaluated by measuring the stimulus threshold to elicit flinching, jumping, and vocalizing in the fear conditioning paradigm and tail flick test.

For mice, cued fear conditioning was conducted in an automated system (Med Associates) via a two conditioned stimulus (CS)-unconditioned stimulus (US) pairings paradigm of 4 min with 60 s intertrial interval. The CS was a tone (75 dB, 8 kHz) coterminating with a mild foot shock US (2 s, 0.7 mA, constant current). Context-dependent conditioning was tested 24 hr later by exposing the mice to the conditioning box for 5 min and tone-dependent freezing was measured at 27 hr by placing the mice in a novel context with novel scent (vanilla) for 3 min pre-CS followed by 3 min CS. Freezing responses were assessed by computer-aided scoring as well as offline manual scoring. For biochemistry and cell surface biotinylation, animals were sacrificed 1 hr after fear conditioning.

Statistical Analyses

All data are represented as mean ± SEM unless stated otherwise. Statistical analysis was performed by the Student's t test unless stated otherwise. For all experiments, *p < 0.05, **p < 0.01, and ***p < 0.001 were considered significant.

SUPPLEMENTAL INFORMATION

Supplemental Information includes Supplemental Experimental Procedures and five figures and can be found with this article online at http://dx.doi.org/10.1016/j.neuron.2014.01.022.

Figure 6. Enhancement of Fear Memory by NR2B siP

(A) Immunostain of rat dorsal hippocampus infused for 24 hr with FITC NR2B siP (green) and counterstained with MAP2 (red). Inset shows FITC-positive CA1 pyramidal neurons. Scale bars represent 250 μm and 50 μm (inset).

(B and C) Immunoblots showing infused NR2B siP versus scramble control reduces P-S1116 (n = 4) (B) and increases NR2B cell surface expression (4 pooled tissue punches for each condition) (C) in epifluorescent hippocampal area CA1.

(D) Experimental design and quantitation of context- and tone-elicited fear memory in 2-month-old rats chronically infused with scrambled or NR2B siP into dorsal hippocampus (n = 20) showing that NR2B siP improved contextual fear memory.

(E) Experimental design and quantitation of fear memory in acutely infused 3-month-old mice. Ninety minutes prior to training, mice were infused with NR2B siP or control peptide into dorsal hippocampus. Twenty-four hours later, NR2B siP-treated mice exhibited improved context freezing, but not freezing to tone (n = 6–10). Data are represented as mean ± SEM. See also Figures S4 and S5.

(F) Model of NR2B regulation via Ser1116 phosphorylation by Cdk5. At basal state, Cdk5 constitutively phosphorylates NR2B at Ser1116, withholding it from the cell surface. Glutamatergic neurotransmission reduces Cdk5-dependent NR2B phosphorylation, enabling translocation of NR2B to the cell surface and thereby contributing to memory formation. Addition of NR2B siP disrupts NR2B-Cdk5 interactions and reduces Ser1116 phosphorylation, and more NR2B translocates to the cell surface, thereby enhancing memory formation.

REFERENCES

Angelo, M., Plattner, F., Irvine, E.E., and Giese, K.P. (2003). Improved reversal learning and altered fear conditioning in transgenic mice with regionally restricted p25 expression. Eur. J. Neurosci. *18*, 423–431.

Angelo, M., Plattner, F., and Giese, K.P. (2006). Cyclin-dependent kinase 5 in synaptic plasticity, learning and memory. J. Neurochem. *99*, 353–370.

Barkus, C., McHugh, S.B., Sprengel, R., Seeburg, P.H., Rawlins, J.N., and Bannerman, D.M. (2010). Hippocampal NMDA receptors and anxiety: at the interface between cognition and emotion. Eur. J. Pharmacol. *626*, 49–56.

Bast, T., Zhang, W.N., and Feldon, J. (2003). Dorsal hippocampus and classical fear conditioning to tone and context in rats: effects of local NMDA-receptor blockade and stimulation. Hippocampus *13*, 657–675.

Bibb, J.A., Snyder, G.L., Nishi, A., Yan, Z., Meijer, L., Fienberg, A.A., Tsai, L.-H., Kwon, Y.T., Girault, J.-A., Czernik, A.J., et al. (1999). Phosphorylation of DARPP-32 by Cdk5 modulates dopamine signalling in neurons. Nature *402*, 669–671.

Bibb, J.A., Mayford, M.R., Tsien, J.Z., and Alberini, C.M. (2010). Cognition enhancement strategies. J. Neurosci. *30*, 14987–14992.

Billard, J.M. (2010). Long-term depression in the hippocampal CA1 area of aged rats, revisited: contribution of temporal constraints related to slice preparation. PLoS ONE *5*, e9843, http://dx.doi.org/10.1371/journal.pone.0009843.

Bliss, T.V., and Collingridge, G.L. (1993). A synaptic model of memory: long-term potentiation in the hippocampus. Nature *361*, 31–39.

Brim, B.L., Haskell, R., Awedikian, R., Ellinwood, N.M., Jin, L., Kumar, A., Foster, T.C., and Magnusson, K.R. (2013). Memory in aged mice is rescued by enhanced expression of the GluN2B subunit of the NMDA receptor. Behav. Brain Res. *238*, 211–226.

Cao, X., Cui, Z., Feng, R., Tang, Y.P., Qin, Z., Mei, B., and Tsien, J.Z. (2007). Maintenance of superior learning and memory function in NR2B transgenic mice during ageing. Eur. J. Neurosci. *25*, 1815–1822.

Chen, B.S., and Roche, K.W. (2007). Regulation of NMDA receptors by phosphorylation. Neuropharmacology *53*, 362–368.

Cingolani, L.A., Thalhammer, A., Yu, L.M., Catalano, M., Ramos, T., Colicos, M.A., and Goda, Y. (2008). Activity-dependent regulation of synaptic AMPA receptor composition and abundance by beta3 integrins. Neuron *58*, 749–762.

Collingridge, G.L., Volianskis, A., Bannister, N., France, G., Hanna, L., Mercier, M., Tidball, P., Fang, G., Irvine, M.W., Costa, B.M., et al. (2013). The NMDA receptor as a target for cognitive enhancement. Neuropharmacology *64*, 13–26.

Cook, D.J., Teves, L., and Tymianski, M. (2012). Treatment of stroke with a PSD-95 inhibitor in the gyrencephalic primate brain. Nature *483*, 213–217.

Craik, D.J., Fairlie, D.P., Liras, S., and Price, D. (2013). The future of peptide-based drugs. Chem. Biol. Drug Des. *81*, 136–147.

Crair, M.C., and Malenka, R.C. (1995). A critical period for long-term potentiation at thalamocortical synapses. Nature *375*, 325–328.

Cull-Candy, S.G., and Leszkiewicz, D.N. (2004). Role of distinct NMDA receptor subtypes at central synapses. Sci. STKE *2004*, re16.

Dhavan, R., and Tsai, L.H. (2001). A decade of CDK5. Nat. Rev. Mol. Cell Biol. *2*, 749–759.

Dingledine, R., Borges, K., Bowie, D., and Traynelis, S.F. (1999). The glutamate receptor ion channels. Pharmacol. Rev. *51*, 7–61.

Fischer, A., Sananbenesi, F., Pang, P.T., Lu, B., and Tsai, L.H. (2005). Opposing roles of transient and prolonged expression of p25 in synaptic plasticity and hippocampus-dependent memory. Neuron *48*, 825–838.

Fujita, Y., Morinobu, S., Takei, S., Fuchikami, M., Matsumoto, T., Yamamoto, S., and Yamawaki, S. (2012). Vorinostat, a histone deacetylase inhibitor, facilitates fear extinction and enhances expression of the hippocampal NR2B-containing NMDA receptor gene. J. Psychiatr. Res. *46*, 635–643.

Gao, X.B., Pellois, J.P., Na, Y., Kim, Y., Gulari, E., and Zhou, X. (2004). High density peptide microarrays. In situ synthesis and applications. Mol. Divers. *8*, 177–187.

Goda, Y., and Colicos, M.A. (2006). Photoconductive stimulation of neurons cultured on silicon wafers. Nat. Protoc. *1*, 461–467.

Guttmann, R.P., Baker, D.L., Seifert, K.M., Cohen, A.S., Coulter, D.A., and Lynch, D.R. (2001). Specific proteolysis of the NR2 subunit at multiple sites by calpain. J. Neurochem. *78*, 1083–1093.

Hawasli, A.H., Benavides, D.R., Nguyen, C., Kansy, J.W., Hayashi, K., Chambon, P., Greengard, P., Powell, C.M., Cooper, D.C., and Bibb, J.A. (2007). Cyclin-dependent kinase 5 governs learning and synaptic plasticity via control of NMDAR degradation. Nat. Neurosci. *10*, 880–886.

Hopkins, A.L., and Groom, C.R. (2002). The druggable genome. Nat. Rev. Drug Discov. *1*, 727–730.

Husi, H., Ward, M.A., Choudhary, J.S., Blackstock, W.P., and Grant, S.G. (2000). Proteomic analysis of NMDA receptor-adhesion protein signaling complexes. Nat. Neurosci. *3*, 661–669.

Jiang, Y., Jakovcevski, M., Bharadwaj, R., Connor, C., Schroeder, F.A., Lin, C.L., Straubhaar, J., Martin, G., and Akbarian, S. (2010). Setdb1 histone methyltransferase regulates mood-related behaviors and expression of the NMDA receptor subunit NR2B. J. Neurosci. *30*, 7152–7167.

Joliot, A., and Prochiantz, A. (2004). Transduction peptides: from technology to physiology. Nat. Cell Biol. *6*, 189–196.

Jubb, H., Higueruelo, A.P., Winter, A., and Blundell, T.L. (2012). Structural biology and drug discovery for protein-protein interactions. Trends Pharmacol. Sci. *33*, 241–248.

Lau, C.G., and Zukin, R.S. (2007). NMDA receptor trafficking in synaptic plasticity and neuropsychiatric disorders. Nat. Rev. Neurosci. *8*, 413–426.

Lee, Y.S., and Silva, A.J. (2009). The molecular and cellular biology of enhanced cognition. Nat. Rev. Neurosci. *10*, 126–140.

Lipinski, C.A. (2000). Drug-like properties and the causes of poor solubility and poor permeability. J. Pharmacol. Toxicol. Methods *44*, 235–249.

Ma, D., and Jan, L.Y. (2002). ER transport signals and trafficking of potassium channels and receptors. Curr. Opin. Neurobiol. *12*, 287–292.

Martin, S.J., Grimwood, P.D., and Morris, R.G. (2000). Synaptic plasticity and memory: an evaluation of the hypothesis. Annu. Rev. Neurosci. *23*, 649–711.

Milner, A.J., Cummings, D.M., Spencer, J.P., and Murphy, K.P. (2004). Bidirectional plasticity and age-dependent long-term depression at mouse CA3-CA1 hippocampal synapses. Neurosci. Lett. *367*, 1–5.

Monyer, H., Burnashev, N., Laurie, D.J., Sakmann, B., and Seeburg, P.H. (1994). Developmental and regional expression in the rat brain and functional properties of four NMDA receptors. Neuron *12*, 529–540.

Morrisett, R. (1997). Electrophysiologic characteristics of heteromeric recombinant NMDA receptors. In The Ionotropic Glutamate Receptors, D.T. Monaghan and R.J. Wenthold, eds. (Totowa: Humana Press).

Mu, Y., Otsuka, T., Horton, A.C., Scott, D.B., and Ehlers, M.D. (2003). Activity-dependent mRNA splicing controls ER export and synaptic delivery of NMDA receptors. Neuron *40*, 581–594.

Myers, S.J., Dingledine, R., and Borges, K. (1999). Genetic regulation of glutamate receptor ion channels. Annu. Rev. Pharmacol. Toxicol. *39*, 221–241.

Nakazawa, K., McHugh, T.J., Wilson, M.A., and Tonegawa, S. (2004). NMDA receptors, place cells and hippocampal spatial memory. Nat. Rev. Neurosci. *5*, 361–372.

Newpher, T.M., and Ehlers, M.D. (2008). Glutamate receptor dynamics in dendritic microdomains. Neuron *58*, 472–497.

Nguyen, C., Nishi, A., Kansy, J.W., Fernandez, J., Hayashi, K., Gillardon, F., Hemmings, H.C., Jr., Nairn, A.C., and Bibb, J.A. (2007). Regulation of protein phosphatase inhibitor-1 by cyclin-dependent kinase 5. J. Biol. Chem. *282*, 16511–16520.

Phillips, R.G., and LeDoux, J.E. (1992). Differential contribution of amygdala and hippocampus to cued and contextual fear conditioning. Behav. Neurosci. *106*, 274–285.

Plattner, F., Angelo, M., and Giese, K.P. (2006). The roles of cyclin-dependent kinase 5 and glycogen synthase kinase 3 in tau hyperphosphorylation. J. Biol. Chem. *281*, 25457–25465.

Pozo, K., Cingolani, L.A., Bassani, S., Laurent, F., Passafaro, M., and Goda, Y. (2012). β3 integrin interacts directly with GluA2 AMPA receptor subunit and regulates AMPA receptor expression in hippocampal neurons. Proc. Natl. Acad. Sci. USA *109*, 1323–1328.

Rush, J., Moritz, A., Lee, K.A., Guo, A., Goss, V.L., Spek, E.J., Zhang, H., Zha, X.M., Polakiewicz, R.D., and Comb, M.J. (2005). Immunoaffinity profiling of tyrosine phosphorylation in cancer cells. Nat. Biotechnol. *23*, 94–101.

Sahin, B., Shu, H., Fernandez, J., El-Armouche, A., Molkentin, J.D., Nairn, A.C., and Bibb, J.A. (2006). Phosphorylation of protein phosphatase inhibitor-1 by protein kinase C. J. Biol. Chem. *281*, 24322–24335.

Scott, D.B., Blanpied, T.A., Swanson, G.T., Zhang, C., and Ehlers, M.D. (2001). An NMDA receptor ER retention signal regulated by phosphorylation and alternative splicing. J. Neurosci. *21*, 3063–3072.

Sheng, M., Cummings, J., Roldan, L.A., Jan, Y.N., and Jan, L.Y. (1994). Changing subunit composition of heteromeric NMDA receptors during development of rat cortex. Nature *368*, 144–147.

Snyder, E.M., Nong, Y., Almeida, C.G., Paul, S., Moran, T., Choi, E.Y., Nairn, A.C., Salter, M.W., Lombroso, P.J., Gouras, G.K., and Greengard, P. (2005). Regulation of NMDA receptor trafficking by amyloid-beta. Nat. Neurosci. *8*, 1051–1058.

Tang, Y.P., Shimizu, E., Dube, G.R., Rampon, C., Kerchner, G.A., Zhuo, M., Liu, G., and Tsien, J.Z. (1999). Genetic enhancement of learning and memory in mice. Nature *401*, 63–69.

Vandenberghe, W., and Bredt, D.S. (2004). Early events in glutamate receptor trafficking. Curr. Opin. Cell Biol. *16*, 134–139.

Wenthold, R.J., Prybylowski, K., Standley, S., Sans, N., and Petralia, R.S. (2003). Trafficking of NMDA receptors. Annu. Rev. Pharmacol. Toxicol. *43*, 335–358.

Wong, R.W., Setou, M., Teng, J., Takei, Y., and Hirokawa, N. (2002). Overexpression of motor protein KIF17 enhances spatial and working memory in transgenic mice. Proc. Natl. Acad. Sci. USA *99*, 14500–14505.

Yin, X., Takei, Y., Kido, M.A., and Hirokawa, N. (2011). Molecular motor KIF17 is fundamental for memory and learning via differential support of synaptic NR2A/2B levels. Neuron *70*, 310–325.

Yuen, E.Y., Wei, J., Liu, W., Zhong, P., Li, X., and Yan, Z. (2012). Repeated stress causes cognitive impairment by suppressing glutamate receptor expression and function in prefrontal cortex. Neuron *73*, 962–977.

Zhang, X.H., Wu, L.J., Gong, B., Ren, M., Li, B.M., and Zhuo, M. (2008). Induction- and conditioning-protocol dependent involvement of NR2B-containing NMDA receptors in synaptic potentiation and contextual fear memory in the hippocampal CA1 region of rats. Mol. Brain *1*, 9, http://dx.doi.org/10.1186/1756-6606-1-9.

Zhao, M.G., Toyoda, H., Lee, Y.S., Wu, L.J., Ko, S.W., Zhang, X.H., Jia, Y., Shum, F., Xu, H., Li, B.M., et al. (2005). Roles of NMDA NR2B subtype receptor in prefrontal long-term potentiation and contextual fear memory. Neuron *47*, 859–872.